

Expendable current profiler (XCP) section across the North Pacific at 25°N

PEARN P. NIILER,* DONG-KYU LEE,* WILLIAM YOUNG* and JIAN-HWA HU†

(Received 12 May 1989; in revised form 2 July 1990; accepted 9 August 1990)

Abstract—In mid-1985, 201 expendable current profiler (XCP) probes were deployed along a track which crossed the North Pacific mostly along latitude 24°15'. About three quarters of the probes provided good data on relative horizontal velocity and temperature. Small vertical scale features in velocity show different characteristics in the California Current, the eastern Pacific and the western Pacific. Spectral energy of the small vertical scale features (WKB stretched wavelength of 20–150 m) increases to the west in rather discrete “jumps” at 153°W, 173°E and 132°E. A simple power law model of spectral energy of this band reveals that the steeper the spectral slope, the larger its amplitude; 20 m wavelength band energy is quite uniform across the ocean. The 150 m vertical-average and horizontal eddy-scale (30–80 km) velocity is nearly geostrophic because the estimated geostrophic currents from the accompanying CTD survey agree very well with XCP currents. The characteristics of eddies in the eastern Pacific are similar to the variability described by NIILER and HALL (1988, *Journal of Physical Oceanography*, **18**, 1670–1685) from moored current meters. The eddy energy also increases to the west. The most surprising finding in these measurements is the strong (order of 10–15 cm s⁻¹) large horizontal scale eastward flow in both the eastern Pacific and the western Pacific. This strong eastward flow has a zonal extent of 1200 km. Other data suggest a meridional extent of 300–400 km.

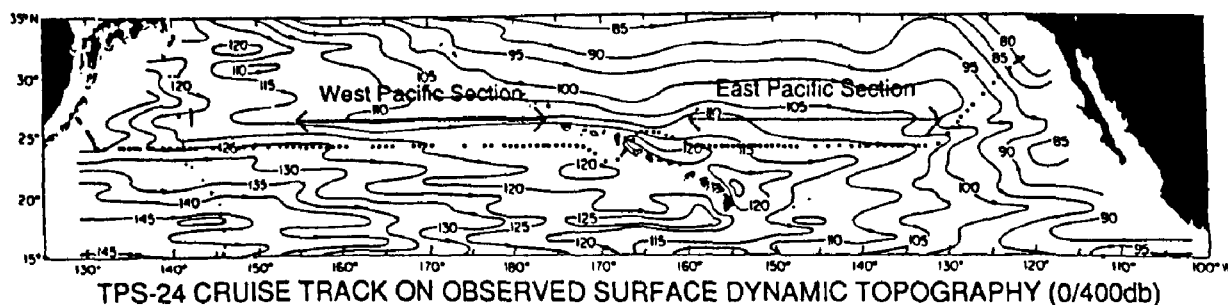
1. INTRODUCTION

DURING April–May 1985, a trans-oceanic hydrographic section was occupied along latitude 24°15'N in the North Pacific with approximately 30' longitudinal sampling. One of the many measurements obtained during that cruise was vertical profiles of horizontal velocity using expendable current profilers (XCP) (manufacturer: Sippican). The XCP stations were positioned near the midpoint between adjacent CTD stations. The purpose of these direct velocity measurements was to obtain the ageostrophic components of the current vectors relative to 1500 db across the section. These data allow us to describe flow structures with vertical wavelengths of 6–750 m in both directions.

This trans-Pacific section, which is now termed TPS-24, is located among some rather interesting circulation features. First, it crosses through the northern segment of the surface dynamic topography of the subtropical gyre where the long-term mean surface geostrophic velocity relative to 400 db is to the southeast (Fig. 1). WYRTKI's (1975) dynamic topography relative to 1500 db places it in the middle of the gyre. The geostrophic hodograph relative to 3000 db calculated from historical data east of Hawaii by LEE and

*Scripps Institution of Oceanography, La Jolla, CA 92093, U.S.A.

†National Taiwan Ocean University, Keelung, Taiwan.



TPS-24 CRUISE TRACK ON OBSERVED SURFACE DYNAMIC TOPOGRAPHY (0/400db)
 Fig. 1. TPS-24 cruise track drawn in the surface dynamic topography from WHITE and WALKER (1985). Two sections used in the analyses are marked. Note that they are in the weak eastward flow region.

NIILER (1987) places TPS-24 in an area of southward or southeastward flow near the surface and southwestward and westward flow at 400 db. According to RODEN (1975), it lies south of the subtropical frontal zone of 28°–33°N. NIILER and REYNOLDS (1984) and HU and NIILER (1987) show that east of the Hawaiian Ridge in the mesoscale eddy energy decreases to the north of TPS-24, and SCHMITZ (1988) shows that eddy energy increases northward toward the Kuroshio Extension west of the dateline.

Besides mesoscale eddy activity, which has scales of 30–80 km in both directions (NIILER and HALL, 1989; BERNSTEIN and WHITE, 1974), curious bands of alternating zonal currents with the same north–south scale as the eddies have been reported along the path of TPS-24. TALLEY and DESZOEKE (1986) report that their eddy-resolving hydrographic section along 152°W shows 60 cm s⁻¹ alternating zonal flows near 25°N which have oxygen anomalies representative of water 1500 km to the west of 152°W. RODEN (1977, 1980) and PRICE (1981) observed similar energetic features in other areas of subtropical gyres which they interpreted as east–west elongated features or frontal zones. In the western Pacific, UDA and HASUNUMA (1969) computed 20 cm s⁻¹ relative eastward geostrophic currents between 23°–25°N along the 137°30'E hydrographic line occupied by the Japanese for many years. YOSHIDA and KIDOKORO (1967) hypothesized that this eastward flow is a result of direct wind forcing by a trough in the anticyclonic wind stress curl. WHITE and WALKER (1985) note that a Sverdrup model of the Pacific with a Hawaiian Islands arc as a barrier has a mid-subtropical gyre counter-current as a semi-permanent feature near 24°N west of the Hawaiian Ridge.

Thus, at the outset we expect our measurements to contain a healthy population of subtropical eddies, large meridional scale zonal flows and, of course, the ubiquitous small-scale variabilities which are thought to be related to internal wave activity. We also expect some differences between the western and eastern ends of the section because the western end crossed through the Kuroshio Current system. In Section 2 we discuss the XCP system and data processing procedures. In Section 3, small vertical scale currents (non-geostrophic motions) are discussed and in Section 4 large vertical scale motions (geostrophically balanced) are discussed. Features of basin-wide scale (500 km horizontal scale)* are presented in Section 5.

* In this paper we use "scale" to designate one sixth of a wavelength and "size" is nominally equal to three scale lengths.

2. DATA PROCEDURE

The XCP (SANFORD *et al.*, 1974) infers ocean currents from the motionally-induced electrical fields caused by a flux of salt ions in the Earth's magnetic field. Horizontally spaced electrodes mounted on a freely falling probe are used to sense the electric current density and these electric current measurements provide a horizontal velocity relative to an unknown but depth-dependent constant velocity. In general, the east-west component is insensitive to the fall rate of the probe, the north-south component depends upon probe fall rate and is computed from the small difference of two large numbers. The detailed operation principle is described in SANFORD (1971) and SANFORD *et al.* (1982).

Vertical resolution of the profiler is quoted as 3 m, and measurement uncertainty is less than 1 cm s^{-1} . Thus, the XCP gives usable velocity profiles for analyses of upper ocean variability. The measurement error increases for high vertical wave number structures, whose high frequency distribution has been described by PINKEL *et al.* (1987) for non-geostrophic motions. We dropped 201 probes, which had a depth range of 1500 m, at every half-way point between adjacent CTD stations. Stations were spaced about 80 km apart over the abyssal plains and about 50 km apart over rougher topography (Fig. 1). Near the eastern and western boundaries the stations were spaced less than 10 km apart. About 25% of the probes failed to produce usable data due to malfunctions which were probe release failures, weak FM signals, seawater battery malfunctions and buoy release failures (Table 1). The critical problem was that many components (e.g. seawater battery, FM transmitter and probe release fuse) could not be tested before deployment.

The successfully collected data were stored on micro floppy diskettes and processed after the cruise. The signal processing program (manufacturer: Sippican) estimates velocity errors and these were used for screening the data. The erroneous data points (error greater than 1 cm s^{-1}) were removed and linearly interpolated. Typical velocity profiles have only a few erroneous points, and these can easily be recognized as spikes (Fig. 2a,b). Figure 2b is a typical temperature and velocity profile in the eastern Pacific. Figure 2a is an unusual profile because it shows strong velocity shear in the mid-depth and a 100 m thick mixed layer centered at 500 m depth. This station is located at $129^{\circ}36'E$ and $25^{\circ}20'N$ and is near the Mariana Trench. An example of a totally noisy profile is presented in Fig. 2c. Noisy stations, with velocity error levels similar to Fig. 2c, were not used in the further analyses. The kinetic energy spectra show that in these bad profiles the noise level is high in all wave number bands (Fig. 3). During the data acquisition, we also recorded the FM signals on a commercial cassette-tape recorder from which we were able to reprocess many stations that had weak FM signals using a Hi-Fi amplifier and a tape player (a technique

Table 1. XCP failure modes during TPS-24 cruise

Serial number	Weak or noisy signal	No FM but strong carrier signal	Probe release failure	FM stopped at the middle of drop	Buoy inflation failure	Operator mistake	Successful drop	Total
1000	3	3	2	9	1	0	58	76
2000	1	0	0	0	1	0	10	12
3000	17	4	7	2	0	2	82	114
Total	21	7	9	11	2	2	150	202

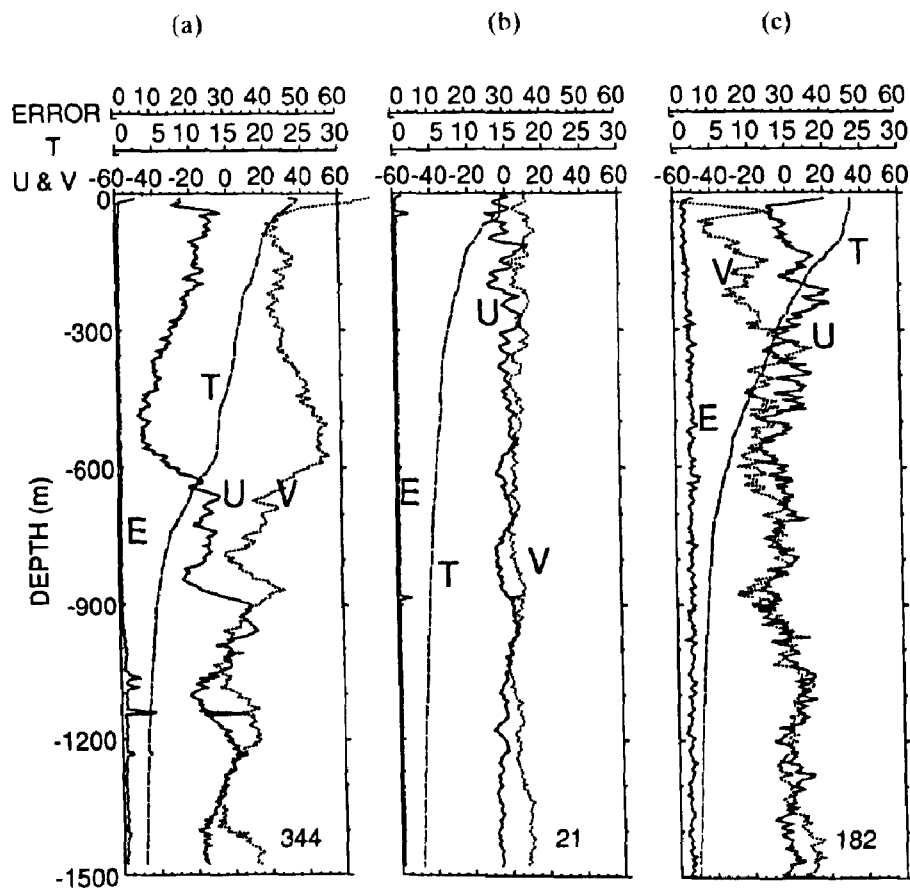


Fig. 2. Typical velocity profiles with temperature from XCP drops in (a) the western Pacific, (b) the eastern Pacific and (c) for a noisy station.

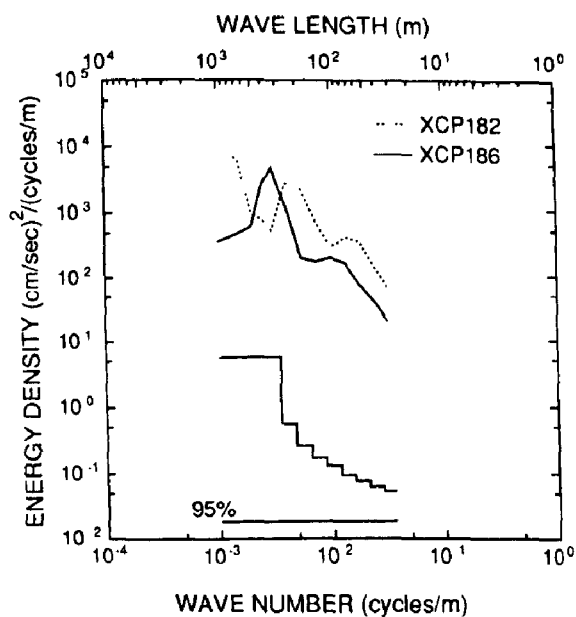


Fig. 3. Energy spectra from profiles at Sta. 186 (solid line) and the noisy station, 182 shown in Fig. 2c (dotted line). Note that the energy of the noisy profile is high in all wave number bands.

recommended to us and used by T. Sanford and his colleagues at University of Washington).

3. SMALL-SCALE FEATURES

The most obvious features of the vertical profiles of horizontal flow are those with vertical wavelengths smaller than 150 m. These are not in geostrophic balance over horizontal scales of 80 km. Some of these energetic features are thought to be internal waves; others, in fact, might be geostrophically adjusted structures of small vertical scale and horizontal scale less than 80 km. Here we seek to characterize them in WKB-scaled units that removed the effects of local changes of amplitude and vertical scale due to the refraction of linear internal waves propagating through a vertically-changing density field. The profiles are normalized by using the local profile of Brünt-Väisälä frequency, $N(z)$, which is calculated using the temperature profile from the XCP and an average salinity profile from two adjacent CTD stations (LEAMAN and SANFORD, 1975). The velocity at each depth is normalized according to

$$\hat{u}(z) = u(z)/[N(z)/N_0]^{1/2} \quad (1)$$

where $\hat{u}(z)$ is the normalized velocity, $u(z)$ is the original velocity, $N(z)$ is the Brünt-Väisälä profile, and N_0 is a reference Brünt-Väisälä frequency. We use $N_0 = 3$ cph in this study.

The new stretched vertical coordinate is

$$N_0 \hat{z} = \int_{-z}^0 N(z') dz' \quad (2)$$

where \hat{z} and z are the stretched and original coordinates, respectively. The stretched profile is interpolated to equally-spaced (10 stretched meters) values. Examples of these

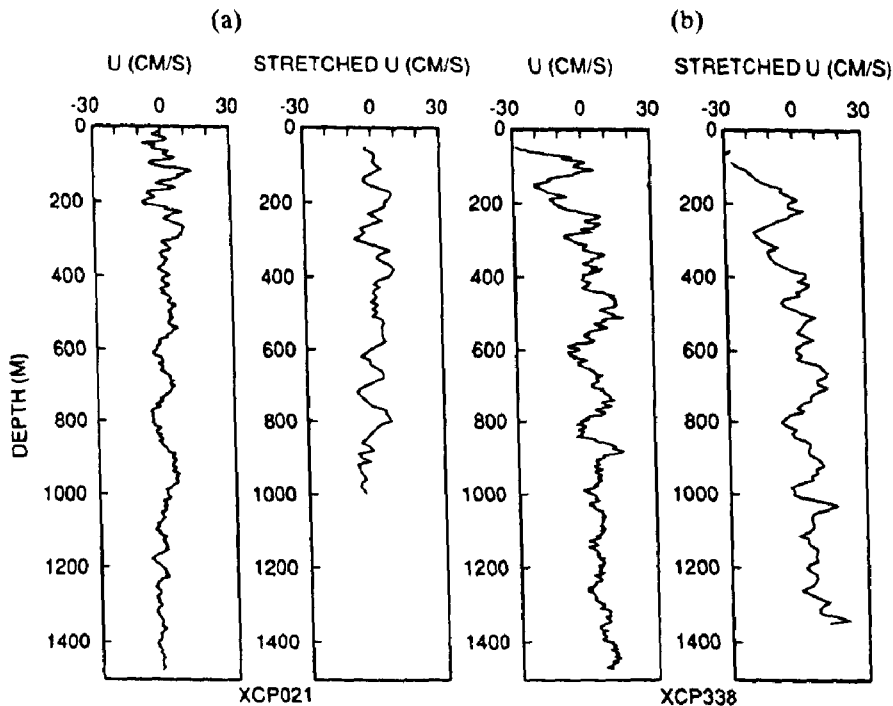


Fig. 4. Profiles of east component for original and stretched velocity (using WKB internal wave scaling) in (a) the eastern Pacific and (b) the western Pacific.

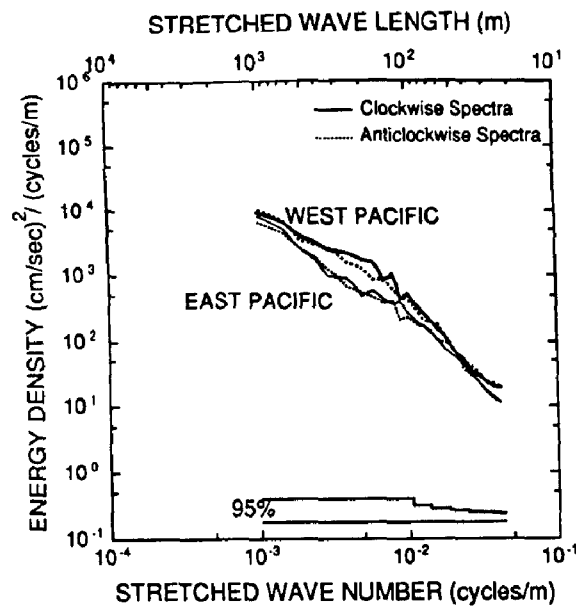


Fig. 5. Rotary spectra after averaging the spectra from 29 XCP profiles in the subtropical Pacific. The solid line is clockwise component and the dashed line is anticlockwise component. The wave number and wavelength are in stretched meters.

new stretched profiles are shown in Fig. 4 together with the original profiles. The stretched profiles appear smoother because of the averaging over 10 m. For comparison, the profiles presented are typical of the eastern Pacific and the western Pacific.

The rotary spectra calculated from 29 stations of the eastern Pacific and the western Pacific are presented in Fig. 5 (the areas from which these come are marked on Fig. 1). The detailed descriptions of the rotary spectra can be found in GONELLA (1972). LEAMAN and SANFORD (1975) found dominance of the clockwise energy spectra as a result of near-inertial waves having downward energy propagation in the MODE area at a particular time. However, in our measurements averaged over broad geographical areas the clockwise energy is the same as the anticlockwise energy in the stretched wave number band (20–200 m). We do not know at this point whether this represents a significant difference between the near-internal wave characteristics of the Atlantic Ocean and the Pacific Ocean or whether this is simply a consequence of the sampling differences (our transect vs Leaman and Sanford's repeated sampling at one location). The spectrum of both clockwise and counterclockwise components of the western Pacific is higher than that of the eastern Pacific in all wave number bands. This result is significant at the 95% confidence level across the entire 50–1000 m band. The higher spectral energies in the west clearly established a regional variability of 20–150 m vertical wavelength structures, a phenomenon that has been known to occur in geostrophic eddy fields (ROEMMICH and MCCALLISTER, 1989). We also computed an ageostrophic component of velocity by subtracting the geostrophic velocity relative to 1000 m from XCP profiles. The spectrum of the ageostrophic component of the velocity normal to the sampling line showed no significant difference from the total spectrum (at 95% confidence level) in the stretched wavelength band of 20–333 m. Only the largest resolved wavelength of 1000 m showed a 60% lower energy level (but not significant at 95% confidence interval) in the ageostrophic component.

For modelling the high wave number structure of individual profiles, we use a simple two parameter representation:

$$E = A(k/k_0)^{-r}, \quad k_0 = 1/150 \text{ cycles m}^{-1}, \quad (3)$$

where k is the vertical wave number and E is the spectral kinetic energy density. Curve fitting in log-log space for wavelengths between 20 and 15 m was applied to individual profiles for values of amplitude, A , and slope, r . In Fig. 6, we present two stations that clearly demonstrate that steeper slopes have larger amplitudes. The amplitudes and slopes for the entire XCP data set are presented in Fig. 7 as a function of the general position along the sampling track. Also presented is the vertically-integrated kinetic energy, which is equal to the sum of the square of the Fourier coefficients in the short wavelength band (20–150 m). The slope varies widely from -1.5 to -3.0 and has an average value of -2.3 . The value in the MODE area is -2.5 (LEAMAN and SANFORD, 1975).

The westward increase of the amplitude, A , is apparent in Fig. 7. The increase is not, however, a gradual one. The spatially-averaged values of this parameter in two regions (the eastern Pacific including the California Current region and the western Pacific region) are also drawn in Fig. 7 with their standard deviations. A similar pattern of westward increase is observed in the mesoscale variability.

Figure 8a shows the scatter plot of average Brünt-Väisälä frequency vs the kinetic energy for the internal wave number band. There is no apparent correlation between \bar{N} and the WKB scaled energy. The scatter plot of amplitude A vs slope r (equation 6) is presented in Fig. 8b. A linear relationship between amplitude and slope is apparent but there is also a clear distinction among the regions: the California Current region, the eastern Pacific and the western Pacific. The least-square fits to individual profiles using a simple power law model reveal that the energy density levels for 20–40 m vertical wavelengths are nearly constant. The energy density level at the 150 m wavelength is not constant between different profiles, increasing significantly from western to eastern Pacific. Thus the spectral level at the 20–40 m wavelength acts as a hinge point and larger values of A correspond to steeper decay (or larger r). Also, when all the spectra are averaged together in both halves of the ocean (Fig. 5), energy density levels in 20–40 m

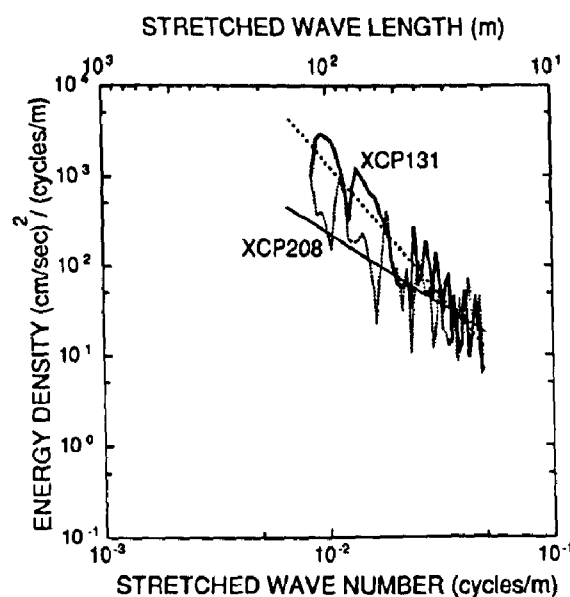


Fig. 6. Example of curve fitting in log-log space using XCP profile and the spectral model discussed in equations (1)–(3).

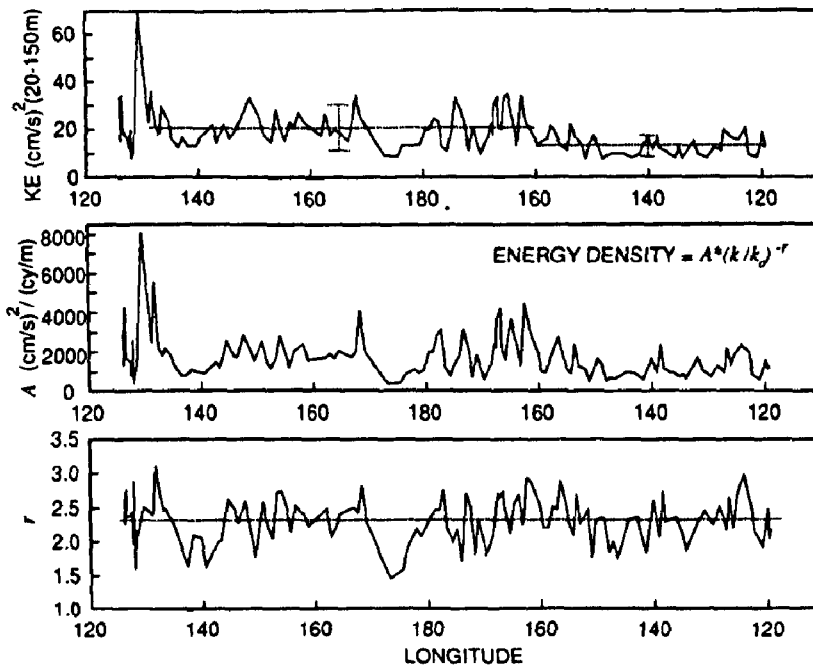


Fig. 7. Kinetic energy in the 20–150 m wavelength band, the amplitude, and the slope from the spectral model, respectively. Dotted lines give the averages and the standard deviations.

wavelengths are indistinguishable across the basin (at 95% confidence). We expected the entire spectral level to increase in regions of high mesoscale activity in the west, but that simply was not borne out by observations: the spectrum just becomes steeper.

In summary, small vertical scale features of the subtropical Pacific Ocean exhibit different characteristics in different regions. The energy is smallest in the California Current region and is largest in the western Pacific. The energy in small wavelengths (20–150 m) increases towards the west, but that increase is not smooth. The energy increase is due to the increased amplitude of small-scale structures and appears even after the removal of the effects of local amplitude and vertical scale change using WKB scaling.

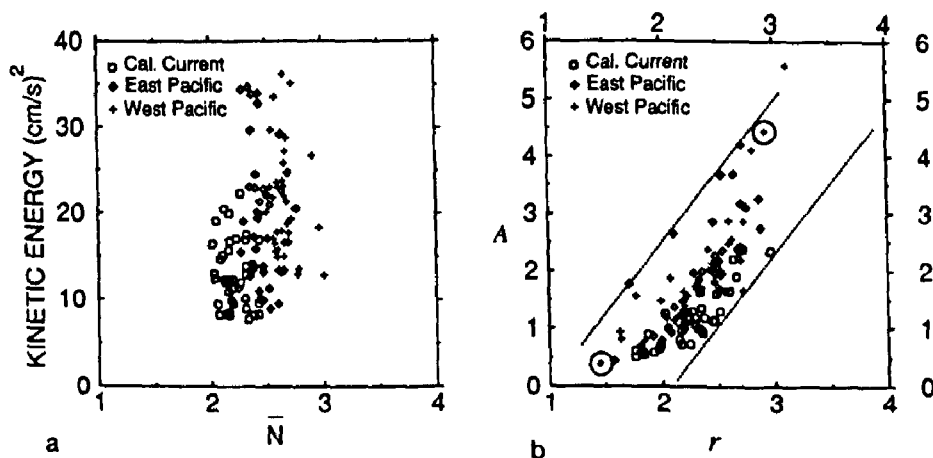


Fig. 8. (a) Kinetic energy of 20–150 m wavelength band as a function of the mean Brunt–Väisälä frequency. (b) The amplitude as a function of slope from the spectral model. The circled stations are those discussed on Fig. 6.

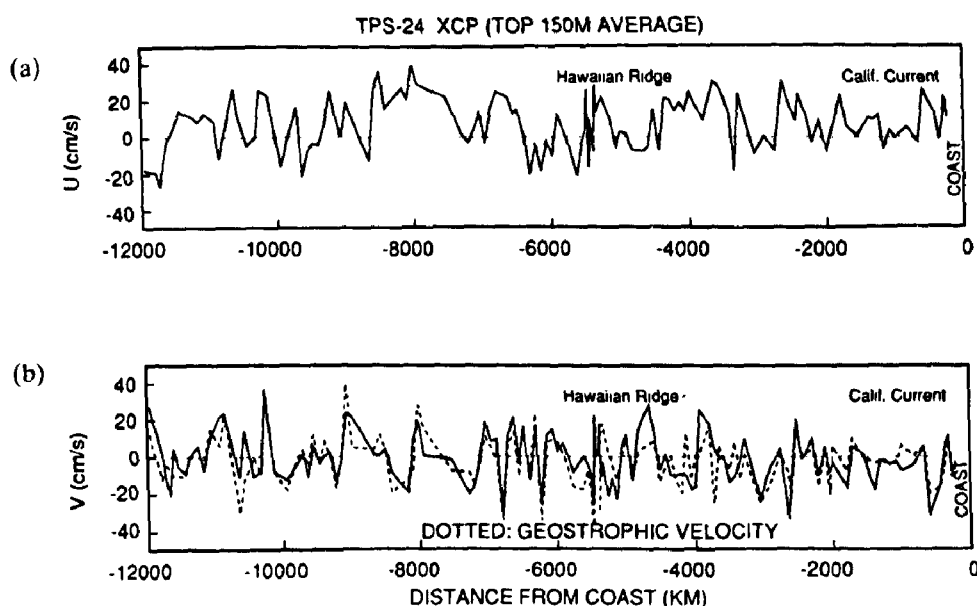


Fig. 9. Vertically averaged velocity of the top 150 m. (a) East-west component from XCP, (b) velocity normal to the section from XCP (solid line) and from geostrophic calculation (dotted line).

4. EDDY FIELD

Little is known about the mesoscale variability in the subtropical North Pacific except its characteristics include a westward propagation and increasing eddy kinetic energy towards the south in the eastern Pacific (HU and NILER, 1987) and an increase to the north in the western Pacific (SCHMITZ, 1988). Our measurement of the velocities along 24°N latitude is the first measurement that makes it possible to compare mesoscale variability of the western and the eastern Pacific along a subtropical latitude. Since the XCP measures total horizontal velocity (not just one component geostrophic value), the total kinetic energy is estimated.

Figure 9 shows the vertically averaged along-track velocities in the top 150 m as measured by the XCP. The velocities normal to the section measured by XCP and the geostrophic velocities calculated from CTD casts are also shown. Both are referenced to a 150 m averaged velocity centered at 1000 m. The XCP and relative geostrophic velocities agree very well on eddy scales except in the area between 3500 km from the California coast and the Hawaiian Ridge. These geostrophic estimates on horizontal scales of 50 km do not agree with the XCP measurement. Either ageostrophic motions on vertical scales of 150 m are strong over this topographic feature, or the geostrophic motions have scales less than 50 km. Except in those areas influenced by topography and those vertical levels affected by wind, the mesoscale variability on 80 km scales in the subtropical Pacific is, as anticipated, nearly geostrophic. Unfortunately there were several XCP failures between 7000 and 9000 km from the California coast and eddies were not well resolved by the XCP in that section.

NILER and HALL (1988) have found that the eddy structures just north of TPS-24 at 28°N, 152°W are characterized by two distinct groups: (1) low frequency eddies having spatial scales of 55–70 km and periods of 100–200 days that propagate southwards and have more zonal than meridional energy, and (2) high frequency eddies having spatial scales of

28–50 km and periods of 40–80 days that are strongly meridionally oriented and propagate southwestward. The station separation in this transoceanic experiment was nearly adequate to resolve those two bands of subtropical eddies in the mid-ocean, but because of numerous XCP failures, we cannot adequately estimate the length scales of the eddies from XCP data. To get an improved quantitative measure of the eddy space scales we obtained the space series of the steric level relative to that at the eastern boundary from ROEMMICH and MCCALLISTER (1989). We used the central 6000 km segment of these data for a description of the eddies. The spectrum of this surface dynamic height is shown in Fig. 10a, graphed in the energy preserving form, as a function of wavelength along the track. The largest contribution to the variance comes from a peak around a wavelength of 512 km, with additional smaller peaks at 365 and 780 km wavelengths. Figure 10b shows the estimate of the relative geostrophic velocity spectrum normal to the sampling line, which is obtained by multiplying the sea-level spectrum estimated on Fig. 10a by gk^2/f . Figure 10b also shows the principal energy containing wavelengths estimated by NIILER and HALL (1989). These latter estimates are obtained from the eastern Pacific, but they also clearly bracket the energy-containing peak for the entire TPS-24. The total variance of the normal component of geostrophic surface velocity (mostly the northward component), as estimated from the sea-level spectrum between the two arrows on Fig. 10b, is $27 \text{ cm}^2 \text{ s}^{-2}$; this is compared to $11 \text{ cm}^2 \text{ s}^{-2}$ as estimated at 304 m depth for the variance of the northward component of velocity at 28°N , 152°W within the same eddy containing band. Since eddy energy in this location increases toward the surface these estimates are comparable. As has been deduced from current meter data and also from numerical models of subtropical eddy fields (see LEE, 1988), multiple and somewhat discrete *temporal* fluctuations exist in the subtropical North Pacific. This eddy-resolving section supports the hypothesis that a number of rather discrete *spatial* scales exist there.

The total kinetic energy of the XCP measurements relative to 1000 m and averaged over upper 150 m is presented in Fig. 11. Surprisingly, the kinetic energy of a few discrete eddies of the eastern Pacific is comparable to that of the western Pacific and these are much larger than the kinetic energy level of the California Current region. The average energy in each area moving westward is 209, 217 and $247 \text{ cm}^2 \text{ s}^{-2}$ and the standard deviation in each area is 217, 157 and $247 \text{ cm}^2 \text{ s}^{-2}$. Since the mean geostrophic current is of the order of 2 cm s^{-1} (LEE and NIILER, 1987) at the surface, the high kinetic energy mainly comes from eddies. There is a slight increase in the kinetic energy level of the eddies from the eastern to the western Pacific. This is also shown by the geostrophically balanced sea-level, relative to sea-level at the eastern boundary, along TPS-24 as presented by ROEMMICH and MCCALLISTER (1989). According to their calculation, the peak to trough amplitude of individual features varies from 40 cm in the Philippine Basin to 5–10 cm in the easternmost 4000 km of the ship track.

To display even larger horizontal scale currents, stick plots for 1000 km running mean velocities in the upper 150 km from the XCP (Fig. 12) show large scale eastward flows in both the eastern and western Pacific with strengths of $10\text{--}20 \text{ cm s}^{-1}$ (see Section 5). Deviations from the 1000 km moving average mean are designated as eddy velocities, scatter plots of which are also shown in Fig. 12 for the California Current, eastern Pacific, Hawaiian Ridge and western Pacific regions. The r.m.s. variance ellipses are drawn in the Hawaiian Ridge and the eastern Pacific areas. The ratio of major and minor axes in the eastern Pacific (1.6:1) is similar to that of the variance ellipse from the three-year-long current meter data of NIILER and HALL (1988) and the rotation angle of the major axis is

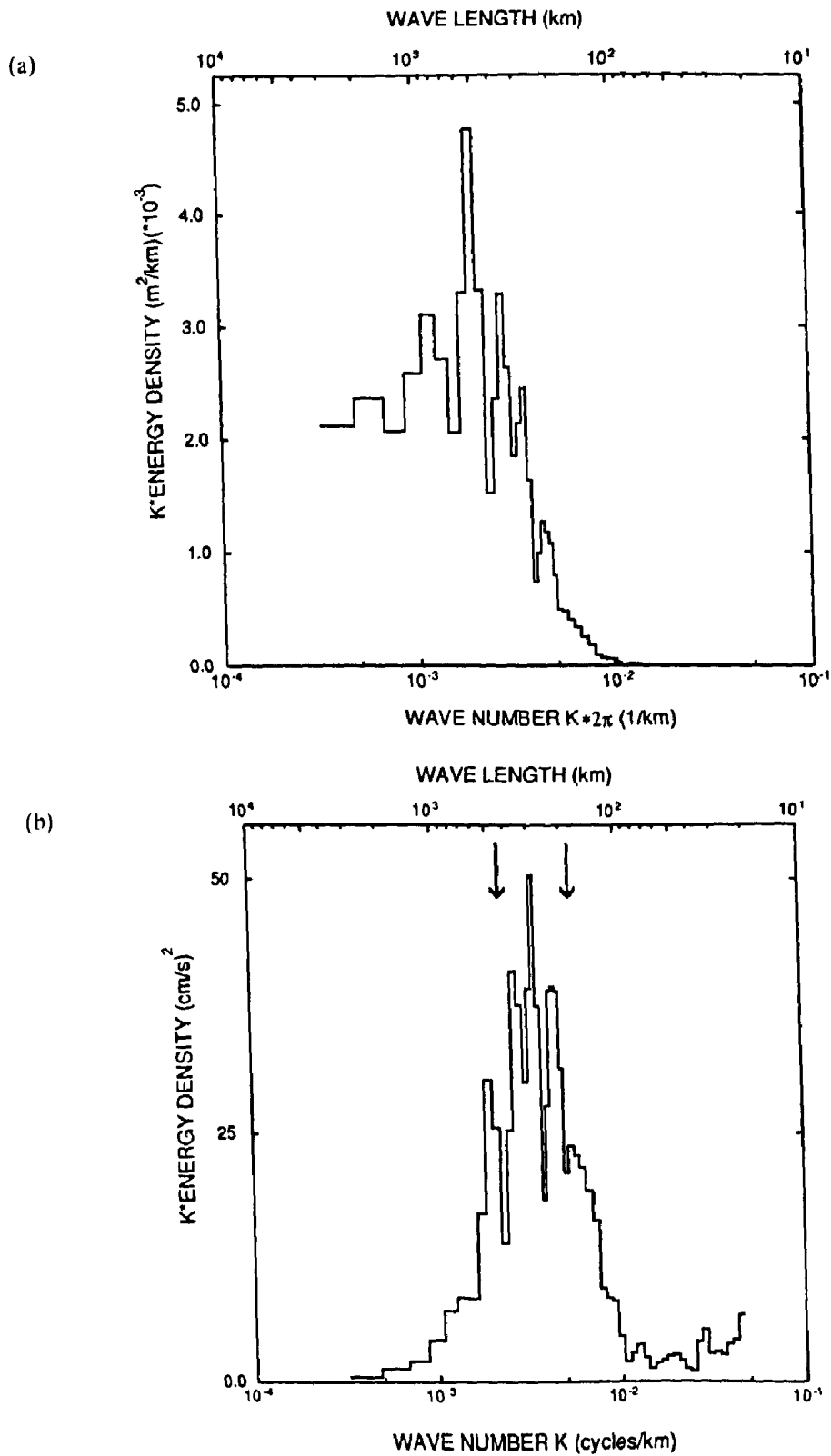


Fig. 10. (a) Energy preserving spectra of the sea-level variability with respect to the eastern boundary calculated from CTD data. (b) Energy preserving spectra of the geostrophic velocity calculated from sea-level spectra. Two predominant waves from NILER and HALL's (1988) current meter mooring data at $152^\circ W$, $28^\circ N$ are marked by arrows.

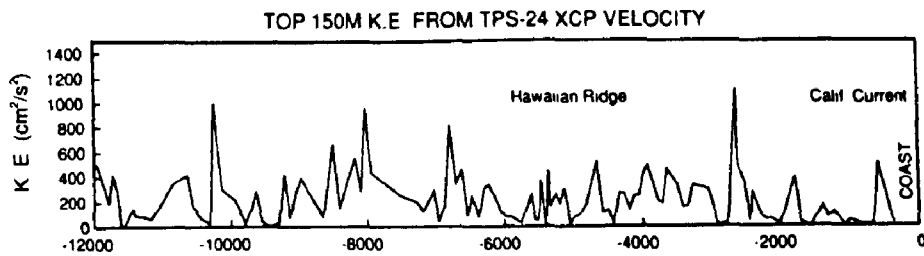


Fig. 11. Kinetic energy as function of distance along TPS-24 calculated from XCP 150 m upper layer vertically averaged velocities.

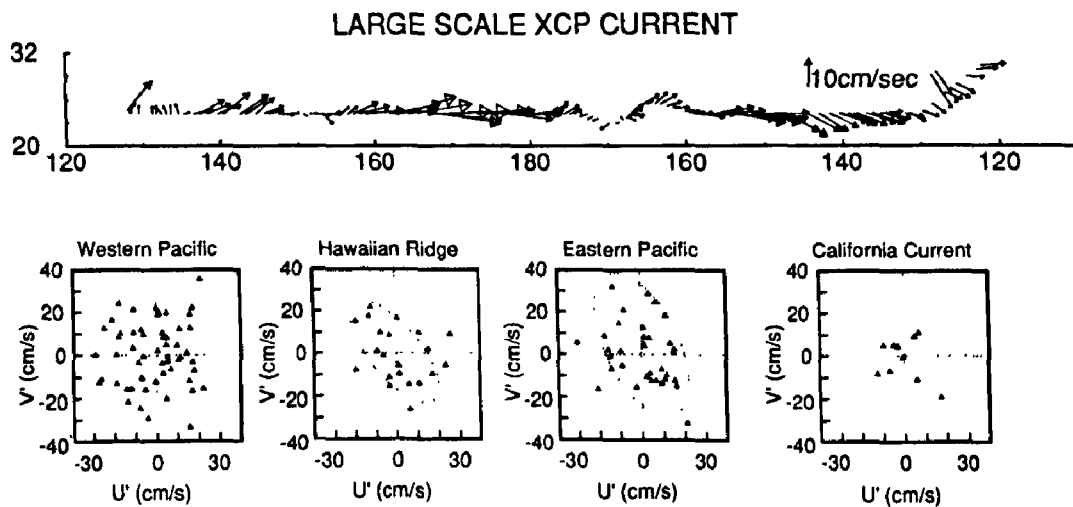


Fig. 12. Stick plots of 1000 km running mean velocities from XCP (upper panel). The lower panel shows the scatter plot of deviations from 1000 km running mean XCP velocities for the California Current (San Diego—130°W), the Eastern Pacific (130°–160°W), the Hawaiian Ridge (160°–172°W) and the Western Pacific (172°W–128°E) region.

close to that of their high-frequency eddies. Of course their velocity data come from a fixed depth (179 m) below our 150 m averaged variance; nevertheless the comparison shows the interesting similarity in the variability of the eastern subtropical Pacific as obtained by these two methods.

The variance plots from the 1000 km running mean for different regions show that the variance of the western Pacific is about 30% larger than that of the eastern Pacific. A clue as to why the mesoscale variability in the western segment is larger than in the eastern segment lies in a further consideration of the depth dependence of the 1000 km spatially averaged mean flow (Fig. 13). The vertical shear of zonal flow in the western section is about 30% larger than that in the eastern section and thus we expect the baroclinic eddy generation process there to be also more vigorous. In numerical models, larger mean zonal shears lead to larger finite amplitude equilibrated eddy fields (LEE, 1988).

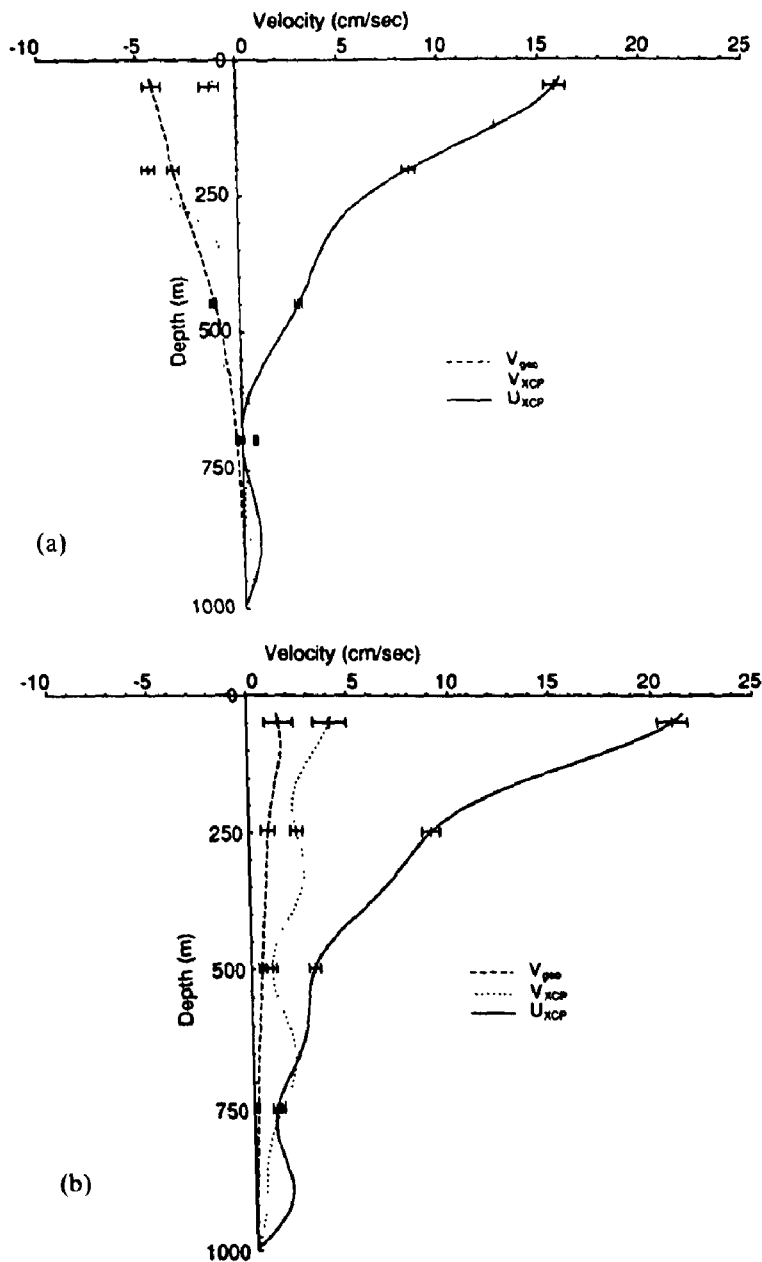


Fig. 13. Horizontally averaged velocity profiles of east component (dashed line), normal velocity to the section from XCP (solid line) and normal geostrophic velocity to the section (dotted line) for (a) the eastern Pacific and (b) the western Pacific. The error of the mean at several depths is also drawn. The profiles used for averaging are the same as in Fig. 5.

5. LARGE HORIZONTAL SCALE FLOW

Figure 14 shows the vertical contours of low-passed eastward flow and northward flow. The filter used was a FIR filter with a rectangular window (OPPENHEIM and SCHAFER, 1975) and a cut-off wavelength of 1200 km. The upper panel shows strong eastward flow in both the eastern Pacific and the western Pacific, except near the Hawaiian Ridge and the Kuroshio Current. The north-south flow contours show a weak southward flow in the eastern Pacific and weak northward flow in the western Pacific. Our estimate of geostrophic current is about twice as large as the estimate from ROEMMICH *et al.* (1991).

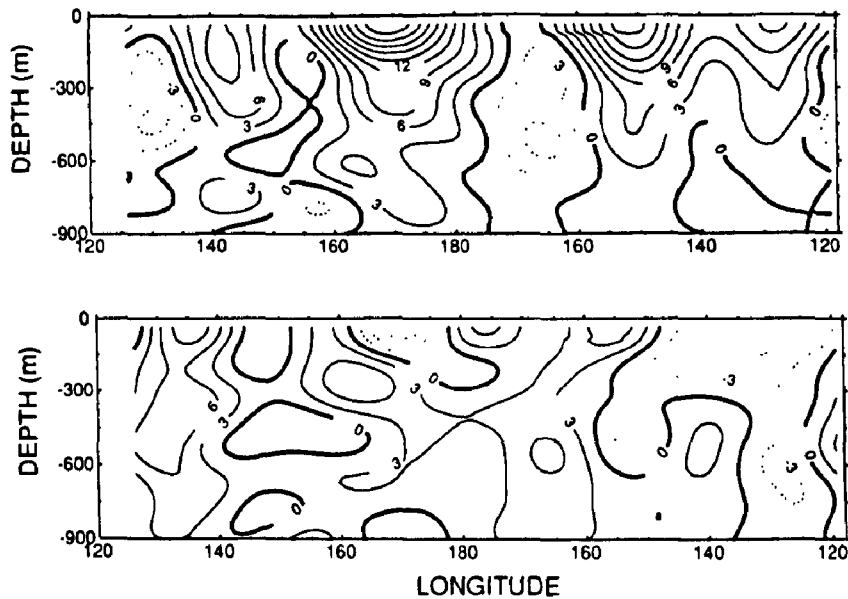


Fig. 14. Vertical and horizontal contours of east–west velocity component (upper panel) and north–south velocity component (lower panel) from low-passed XCP profiles.

This is caused by the failure of two XCPs at stations where there was a strong northward flow (we only calculate the geostrophic current at the successful XCP stations).

Figure 13a displays the average vertical profiles of meridional velocity taken from 30 XCP casts to the east of Hawaii, after filtering out vertical scales less than 150 m (the low pass filter used here is the FIR filter using rectangular window). The XCP profile is similar to the meridional geostrophic profile which is also shown except that the XCP profile has vertical structure which is significant and which does not average out horizontally. We are puzzled by this observation—are there semi-permanent jets in the flow of such large meridional scale? Our data suggest this. The zonal velocity profile shows a stronger eastward flow than the historical geostrophic flow (see Fig. 1 in LEE and NIILER, 1987). This kind of strong eastward flow was observed by TALLEY and DESZEOKE (1986) who concluded from water mass analysis that it is not an eddy with similar east–west and north–south scales but a “semi-permanent” feature due to the presence of the Hawaiian Ridge. The size of such a feature from their analysis is about 800 km zonally and 390 km meridionally. The zonal extent of the eastward flow from our data is about 1000–1200 km (Fig. 9).

We believe that these eastward flows are non-steady. Figure 15 shows the time plot and progressive vector diagram of the current meter moored at 179 m at 28°N and 152°W during 1984. There is a big burst of eastward deflection which started in the middle of May 1984 and ended with a big westward flow in December 1984. The horizontal distance on this progressive vector diagram to the east is about 700 km, which is commensurate with the distance over which oxygen anomalies should have propagated in this area. TALLEY and DESZEOKE (1986) found that the westward flow has lower oxygen content than the eastward flow in the layer between 100 and 300 m (the layer above the abrupt decrease in oxygen). Since the eastward flow to the east of Hawaii observed in this data set shows similar features to the eastward flow which was observed in 1984 by HU and NIILER (1987) and TALLEY and DESZEOKE (1987), we suggest that besides mesoscale eddies of 30–80 km

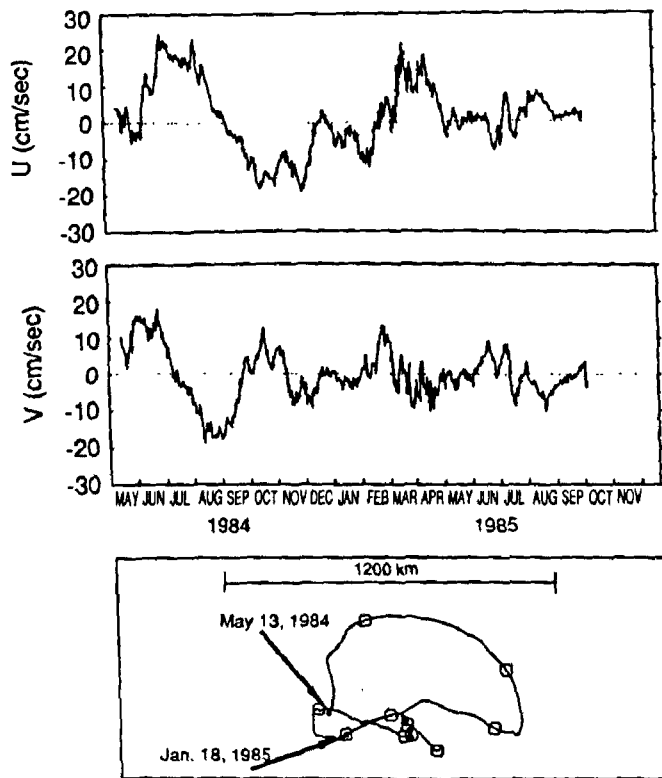


Fig. 15. Time series of the current meter at 194 m at 28°N , 152°W and the corresponding progressive vector diagram (HU and NILLER, 1987).

scale in both directions, there exists comparable amplitude time-dependence motions in the subtropical Pacific that have comparable north–south scales to meso-scale eddies, but much larger east–west scales. We hypothesize long, “sausage-like” structures which move slowly in the subtropical ocean and which have periods in excess of six months. These become unstable from time to time and mesoscale eddies are created in their instability (see NILLER and HALL, 1988 for specific dynamics), or perhaps these sausages are created by rectification of mesoscale eddies. In the upper layers of the western North Atlantic SCHMITZ (1978) has termed these motions “secular scale east–west flows”, so we suggest that they be called “secular sausages”. Barotropic, elongated structures are found in Cox’s (1987) GCM of a North Atlantic-size ocean where they are produced by baroclinic eddy rectification along contours of constant Coriolis parameter.

Another surprising feature is the extent of the strong eastward flow west of Hawaii (Fig. 13b). According to YOSHIDA and KIDOKORO (1967), there is a subtropical countercurrent in the western Pacific which, theoretically, could be formed by a trough in the anticyclonic wind stress curl which is found near the boundary between the Trades and the Westerlies. They have presented observational evidence of the eastward flow, which is located between 20° and 25°N and has geostrophic speeds of $20\text{--}50\text{ cm s}^{-1}$ relative to 1000 m.

In conclusion, our “secular sausages”, have time scales in excess of a few months, have zonal scales of more than 400 km and meridional scales of 30–80 km. “Secular sausages” and mesoscale eddies are inexorably interrelated in the eddy conversion of available potential energy to eddy kinetic energy. They are one of the most recently discovered features of subtropical ocean variability.

Acknowledgements—This research was supported by the Office of Naval Research. We gratefully acknowledge the contribution of Bob Drever at Applied Physics Laboratory of University of Washington, the assistance of Richard G. Allan at sea and Dean Roemmich for the hydrographic data.

REFERENCES

- BERNSTEIN R. L. and W. B. WHITE (1974) Time and length scales of baroclinic eddies in the central North Pacific Ocean. *Journal of Physical Oceanography*, **4**, 613–624.
- COX M. D. (1987) An eddy-resolving numerical model of the ventilated thermocline: time dependence. *Journal of Physical Oceanography*, **17**, 1044–1056.
- FU L.-L., D. B. CHELTON and V. ZLOTNICKI (1988) Satellite altimetry: observing ocean variability from space. *Oceanography*, **1**(2), 4–11.
- GONELLA J. A. (1972) Rotary-component method for analysing meteorological and oceanographic vector time series. *Deep-Sea Research*, **19**, 833–846.
- HU J.-H. and P. P. NIILER (1987) NEPAC current meter and XBT data for the circulation in the northeast Pacific thermocline; 42°N and 28°N, 152°W; July 1982–October 1985. SIO Ref. No. 87-4 (Technical Report).
- LEAMAN K. D. and T. B. SANFORD (1975) Vertical energy propagation of inertial waves: a vector spectral analysis of velocity profiles. *Journal of Geophysical Research*, **80**, 1975–1978.
- LEE D.-K. (1988) A numerical study of the nonlinear stability of the eastern ocean circulation. *Journal of Geophysical Research*, **93**, 10630–10644.
- LEE D.-K. and P. P. NIILER (1987) The local baroclinic instability of geostrophic spirals in the eastern North Pacific. *Journal of Physical Oceanography*, **17**, 1366–1377.
- NIILER P. P. and M. M. HALL (1988) Low frequency eddy variability in the eastern North Pacific subtropical gyre. *Journal of Physical Oceanography*, **18**, 1670–1685.
- NIILER P. P. and R. W. REYNOLDS (1984) The three-dimensional circulation near the eastern North Pacific subtropical front. *Journal of Physical Oceanography*, **14**, 217–230.
- OPPENHEIM A. V. and R. W. SCHAFER (1975) *Digital signal processing*. Prentice-Hall, New Jersey, 585 pp.
- PINKEL R., A. J. PLUEDDEMANN and R. G. WILLIAMS (1987) Internal wave observations from Flip in Mildex. *Journal of Physical Oceanography*, **17**, 1737–1757.
- PRICE J. M. (1981) Monthly mean sea level fluctuations at Honolulu and San Francisco and the intervening geostrophic currents. *Journal of Physical Oceanography*, **11**, 1375–1382.
- RODEN G. I. (1975) On North Pacific temperature, salinity sound velocity and density fronts and their relation to the wind and energy flux fields. *Journal of Physical Oceanography*, **5**, 557–571.
- RODEN G. I. (1977) On long-wave disturbances of dynamic height in the North Pacific. *Journal of Physical Oceanography*, **7**, 41–49.
- RODEN G. I. (1980) On the subtropical frontal zone north of Hawaii during winter. *Journal of Physical Oceanography*, **10**, 342–263.
- ROEMMICH D. and T. MCCALLISTER (1989) Large scale circulation of the North Pacific Ocean. *Progress in Oceanography*, **22**, 171–204.
- ROEMMICH D., T. MCCALLISTER and J. SWIFT (1991) A transpacific hydrographic section along latitude 24°N: the distribution of properties in the subtropical gyre. *Deep-Sea Research*, **38** (Suppl.), S1–S20.
- SANFORD T. B. (1971) Motionally induced electric and magnetic fields of the sea. *Journal of Geophysical Research*, **76**, 3476–3492.
- SANFORD T. B., R. G. DREVER and J. H. DUNLAP (1974) The design and performance of a free-fall electromagnetic velocity profiler (EMVP). Ref. 74-46, Woods Hole Oceanographic Institution, Woods Hole, MA.
- SANFORD T. B., R. G. DREVER, J. H. DUNLAP and E. A. D'ASARO (1982) Design, operation and performance of an expendable temperature and velocity profiler (XTVP). Applied Physics Laboratory, University of Washington, Technical Report APL-UW 8110.
- SCHMITZ W. J. Jr (1978) Observations of the vertical distribution of low frequency kinetic energy in the western North Atlantic. *Journal of Marine Research*, **36**, 295–310.
- SCHMITZ W. J. Jr (1988) Exploration of the eddy field in the midlatitude North Pacific. *Journal of Physical Oceanography*, **18**, 459–468.
- TALLEY L. D. and R. A. DESZEOKE (1986) Spatial fluctuations north of the Hawaiian Ridge. *Journal of Physical Oceanography*, **16**, 981–984.
- UDA M. and K. HASUNUMA (1969) The eastward subtropical countercurrent in the western North Pacific Ocean. *Journal of the Oceanographic Society of Japan*, **25**, 201–210.

-
- WHITE W. B. and T. WALKER (1985) The influence of the Hawaiian Archipelago upon the wind-driven subtropical gyre in the Western North Pacific. *Journal of Geophysical Research*, **90**, 7061–7074.
- WYRTKI K. (1975) Fluctuation of the dynamic topography in the Pacific Ocean. *Journal of Physical Oceanography*, **5**, 450–459.
- YOSHIDA K. and T. KIDOKORO (1967) A subtropical countercurrent (II)—a prediction of eastward flows at lower subtropical latitudes. *Journal of the Oceanographical Society of Japan*, **23**, 231–246.